A Robust, Multi-Solution Framework for Well Placement and Control Optimization

Authors: Mohammad Salehian[1], Morteza Haghighat Sefat[1], Khafiz Muradov[1]*

[1] Institute of GeoEnergy Engineering, Heriot-Watt University, Edinburgh EH14 4AS, United Kingdom

** Corresponding author (Mohammad Salehian), Email: ms315@hw.ac.uk*

ORCID of the authors:

Mohammad Salehian: 0000-0003-4073-292X

Morteza Haghighat Sefat: 0000-0002-6868-4897

Khafiz Muradov: 0000-0003-1587-6964

This is a peer-reviewed, accepted author manuscript of the following article: Salehian, M., Sefat, M. H., & Muradov, K. (2022). A robust, multi-solution framework for well placement and control optimization. Computational Geosciences, 26, 897–914. https://doi.org/10.1007/s10596-021-10099-2

A Robust, Multi-Solution Framework for Well Placement and Control Optimization

Mohammad Salehian, Morteza Haghighat Sefat, Khafiz Muradov

Institute of GeoEnergy Engineering, Heriot-Watt University, Edinburgh EH14 4AS, UK

1. Abstract

Field development and control optimization aim to maximize the economic profit of oil and gas production while considering several sources of uncertainty. This results in a high-dimensional optimization problem with a computationally demanding and uncertain objective function based on the simulated reservoir model. The limitations of many current robust optimization methods are: 1) it is single-level optimization (e.g. optimization of well locations/placement only; or of well production/injection control variables only) that ignores interference between the control variables from different levels; and 2) they provide a single optimal solution, whereas operational problems often add unexpected constraints likely to reduce that optimal, inflexible solution to a sub-optimal scenario.

This paper presents a robust, multi-solution framework based on sequential iterative optimization of control variables at multiple levels using the Simultaneous Perturbation Stochastic Approximation (SPSA) optimization algorithm. A systematic realization selection process, tailored to the objective of the subsequent optimization stage, is used to select a small representative ensemble of reservoir model realizations to be used for calculating the expected objective value. The estimated gradients are calculated using a 1:1 ratio mapping ensemble of control variables perturbations at each iteration onto the ensemble of selected reservoir model realizations to reduce the computational cost. An ensemble of close-to-optimum solutions is then chosen from each level (e.g. from the well placement optimization level) and transferred to the next level of optimization (e.g. where the control settings are optimized), and this loop continues until no significant improvement is observed in the expected objective value. Fit-for-purpose clustering techniques are developed to systematically select an ensemble of solutions, with maximum differences in control variables but close-to-optimum objective values, at each optimization level.

The proposed framework has been tested on a benchmark case study (Brugge field). Multiple solutions are obtained with different well locations and control settings but close-to-optimum objective values. We show that suboptimal solutions from an early optimization level can approach and even outdo the optimal one at the next level(s). Results demonstrate the advantage of the developed framework in more efficient exploration of the search space and providing the much-needed operational flexibility to field operators.

Keywords: robust optimization, well placement, optimal control, SPSA, geological uncertainty

2. Introduction

Optimal field development and management process operates critical decision variables (a.k.a. control variables), such as well locations and control settings, to maximize the economic profit from oil and gas production. However, mathematically this often results in a high-dimensional, constrained optimization problem with computationally demanding and uncertain objective function (i.e. the production forecast model and field performance estimation based on it). The control variables in this optimization problem can be grouped based on their type (e.g. integer, model grid cell number-based well locations; continuous well production/injection pressure or rate control settings, etc.). In this paper we refer to optimization of different variable types as different *'optimization levels'*, e.g. the well location optimization is one level, and the well production/injection control optimization is another level.

Single-level optimization frameworks have been developed to optimize only one type of control variables, such as well locations [1-7] or well control settings like flow rate or pressure [8-18]. These methods may not be appropriate where the optimization problem involves multiple levels, as they do not capture the potential correlations or interference among control variables at different levels. In contrast, multi-level frameworks aim to simultaneously optimize multiple types of variables at different levels to account for the correlation among control variables. Current multi-level approaches can be classified into two groups: (1) Joint optimization [19-21]: this approach optimizes a single augmented vector containing all control variables at different levels. Although the obtained solution using this approach is theoretically optimal, however, a sub-optimal performance as a result of convergence to a local optima is expected when using this approach in reasonable-scale full-field applications due to the optimization algorithm's high demand for computational resources because of the large number of simultaneous control variables [22]. (2) sequential optimization [22-24]: in this approach, the main problem is divided into sub-problems with reduced number of control variables. Each sub-problem is a single-level optimization (with a single type of control variable); an iterative approach is then employed to account for the correlations among control variables at different levels.

Current field development/control optimization frameworks can further be classified into three main groups based on the employed optimization algorithm: (1) stochastic derivative-free and metaheuristic algorithms such as genetic algorithm (GA) [25, 26] or particle swarm optimization (PSO) algorithm [27], (2) adjoint gradient-based algorithms [28-32], and (3) stochastic approximated gradient-based algorithms such as Simultaneous Perturbation Stochastic Approximation (SPSA) [23] or Stochastic Simplex Approximate Gradient (StoSAG) method [33]. Stochastic derivative-free and metaheuristic algorithms can globally search for the optimal solution of all types of control variables (e.g. categorical, integer, continuous), however, they typically have a slower convergence rate than gradient-based algorithms and their performance decreases rapidly when the number of control variables increase [34]. Adjoint gradient-based methods are computationally efficient; however, most of the commercial simulators either do not have a fully developed adjoint code or do not allow access to the source code for efficient calculation of the gradient [35]. Approximate gradient-based algorithms are developed to address this issue by stochastically estimating the gradient of a black-box objective function using an ensemble of simultaneous perturbation of all control variables. The approximate gradient-based algorithms have been successfully employed to solve large-scale well placement (e.g. using SPSA [36]) and well control problems (e.g. using SPSA [37] and StoSAG [38]).

The reservoir model is never perfect, nor the production forecast based on it. Hundreds of reservoir model realizations are generally developed to quantify the underlying uncertainty due to limited reservoir description knowledge. A robust, optimal well placement/control solution can then be achieved by optimizing the expected value of the objective function over the ensemble of model realizations. A variety of techniques have been developed to select a relatively small ensemble of model realizations, as the sufficient representatives of all possible realizations for the problem at hand, to reduce the computation time associated with the robust optimization process. Random sampling of realizations has previously been employed by Guyaguler and Horne [39] and Chen, Li [40], however, random sampling approaches in general cannot guarantee to capture the underlying uncertainty. Iteratively updating the randomly selected samples during the optimization process (e.g. [22, 41]) can potentially improve the performance especially with a large number of iterations. A systematic selection technique [2, 37, 42] is preferred to select a subset of realizations as the representative of all realizations, tailored to the objective of the subsequent optimization.

Current single/multi-level optimization frameworks provide a single solution as the output, while in practice, operational problems often impose unexpected constraints that result in operators having to adjust the optimal solution degrading its value. For instance, the provided optimal well location solution could be impractical (or difficult) to drill, due to the deviation of the well trajectory from the planned trajectory, caused by operational/tool errors. Hence, operational flexibility is an outstanding challenge to be addressed for practical application of the optimization frameworks. This paper presents a multi-solution optimization framework (MSOF) to solve well placement and control problems under geological uncertainty, based on a multi-level sequential (iterative) approach [3]. SPSA is used as the optimizer following previous works proving its efficiency in large-scale problems [23, 43-45]. The gradients at each iteration are stochastically estimated using a 1:1 ratio between the ensemble of control variables perturbations and the ensemble of selected model realizations. An ensemble of close-to-optimum solutions is then chosen from each level (e.g. from the well placement optimization level), transferred to the next level of optimization (e.g. where the well controls are optimized), and this loop continues until no significant improvement is observed in the expected objective value. Fit-for-purpose clustering procedures are developed to systematically select an ensemble of realizations to capture the underlying model uncertainties, as well as an ensemble of solutions with adequate differences in control variables but close-to-optimum objective values, at each optimization level.

Multi-objective optimization approaches, such as bi-objective (pareto front) [16, 18, 46] and hierarchical approaches [29, 35, 40], have been initially used to achieve a secondary objective (usually a short-term gain, e.g. highly discounted cash flow) while maintaining a long-term, primary objective (e.g. undiscounted cash flow). The pareto front approach follows a similar concept to provide a reasonable degree of freedom to the decision maker to choose the optimal solution based on the relative importance of each of the two objectives [16]. The focus of this work is to develop a framework to provide the required operational flexibility in single-objective optimization problems.

This paper is organized as follows: First, problem formulation for robust well placement/control optimization, with an uncertain reservoir model, is presented; followed by a brief description of the SPSA algorithm. Next, the developed techniques for reservoir model realization selection are presented and compared with the alternative realization selection strategies. The MSOF along with the developed techniques for selecting representative solutions at each optimization level are presented. The MSOF is then applied to a benchmark case study (Brugge oil field model). The numerical results are compared with single solution optimization approach and the previous approach of using all the selected realizations for gradient estimation (instead of the proposed 1:1 approach), and the conclusions are drawn.

3. Problem statement

In this work, the objective is to find the optimal set(s) of control variables (i.e. well locations and control settings) to maximize an objective function. Net Present Value (NPV), considering only oil and water production/injection over the presumed life of the reservoir, is the selected objective function, defined as:

$$J(x,m)=\sum_{n=1}^{S}\left\{\left[\sum_{j=1}^{N_P}\left(r_o q_{o,j}^{n}-r_{pw}q_{w,j}^{n}\right)-\sum_{k=1}^{N_I}\left(c_{wi}q_{wi,k}^{n}\right)\right]\times\frac{\delta t^{n}}{(1+b)^{t_n}}\right\} \tag{1}$$

where x is the N_x dimensional vector of the control variables, m is the N_m dimensional vector of the uncertain reservoir description properties (e.g. porosity and permeability fields, fault transmissibility, oil-water contacts) quantified as the reservoir model realizations, n is the n^{th} time step of the reservoir simulation, S is the total number of simulation steps, δt^n is the length of n^{th} simulation step, t_n is the simulation time at the end of the n^{th} time step, b is the annual discount rate in decimal, and N_P and N_I are the number of producers and injectors, respectively. The cost coefficients r_o, r_{pw}, and c_{wi} denote the oil price, the water handling cost, and the water injection cost respectively; all in (USD/STB). $q_{o,j}^{n}$ and $q_{w,j}^{n}$ are the oil and water production rates of well j at time step n in STB/day. $q_{wi,k}^{n}$ is the water injection rate of well k at time step n in STB/day. The expected value of the objective function (J_E) over an ensemble of reservoir model realizations is maximized in order to account for the reservoir description uncertainties. Hence the robust optimization problem is defined as

$$\max_{x\in\mathbb{R}^{N_x}} J_E(x)=\frac{1}{N_r}\sum_{k=1}^{N_r}J(x,m_k) \tag{2}$$

$$subject\ to\ x_i^{min}\le x_i\le x_i^{max}\ ,i=1\ ,2\ ,\dots,N_x \tag{3}$$

where N_r denotes the number of representative reservoir model realizations, m_k represents the N_m dimensional vector of the uncertain reservoir description properties (e.g. porosity and permeability fields, fault transmissibility, oil-water contacts) for the realization k and x_i^{min} and x_i^{max} are the lower and upper bound for the i^{th} component of the control variable vector x, respectively. In this study, control variables x are scaled from the original domain $[x_{min},x_{max}]$ to [0,1] (Eq. (4)) to eliminate the impact of different ranges of control variables at different optimization levels.

$$u_i=\frac{x_i-x_{min,i}}{x_{max,i}-x_{min,i}} \tag{4}$$

Simulation runs are conducted using a commercial reservoir simulator (ECLIPSE-100) [47] to calculate the objective function for the specified set of control variables and model realizations.

3.1. Optimization methodology

SPSA is a stochastic optimization algorithm based on the steepest ascent (or descent) while gradient is approximated using a randomly selected stencil [48]. Consider $J(u_k)$ to be the objective value, where u_k is the N_x dimensional vector of the scaled control variables at iteration k. The gradient $g_k(u)$ is defined as the partial derivatives of the objective function $g_k(u)=\frac{\partial J}{\partial u}=\left[\frac{\partial J}{\partial u_1},\frac{\partial J}{\partial u_2},\dots,\frac{\partial J}{\partial u_{N_x}}\right]^T$, where $[.]^T$ represents a column vector [49]. SPSA iteratively maximizes the objective function $J(u)$ using:

$$u_{k+1}=u_k+\alpha_k\hat{g}_k(u_k) \tag{5}$$

where $\hat{g}_k(u_k)$ is the stochastically estimated gradient of the objective function and $\alpha_k > 0$ is the step size at iteration k. To calculate $\hat{g}_k(u_k)$, $\Delta_k = \left\{\Delta_{k_1}, \Delta_{k_2}, \ldots, \Delta_{k_{N_x}}\right\}$ is defined as a random vector of symmetrically distributed ± 1 values, satisfying the conditions defined by Spall [48]. The stochastic gradient $\hat{g}_k(u_k)$ is then calculated using Δ_k and a positive scalar c_k:

$$\hat{g}_k(u_k) = \frac{J(u_k + c_k\Delta_k) - J(u_k - c_k\Delta_k)}{2c_k} \times \left[\frac{1}{\Delta_{k_1}}, \frac{1}{\Delta_{k_2}}, \ldots, \frac{1}{\Delta_{k_{N_x}}}\right]^T \tag{6}$$

The convergence of the SPSA algorithm depends on the tuning parameters α_k and c_k. Spall [49] suggested the following decaying sequences to calculate α_k and c_k to ensure a gradually refining search:

$$\alpha_k = \frac{a}{(\mathbb{A} + k + 1)^{\vartheta}} \tag{7}$$

$$c_k = \frac{c}{(k+1)^{\gamma}} \tag{8}$$

where a, c, $\mathbb{A}$, ϑ, and γ are positive, real numbers. The values of ϑ and γ are recommended to be 0.602 and 0.101 [48]. The stability constant $\mathbb{A}$ is recommended to be 5-10% of the expected, or allowed, number of iterations when optimizing continuous variables [50]. Jesmani, Jafarpour [41] recommended using a larger $\mathbb{A}$ (e.g. $\mathbb{A}$ was set to 100 that is 33.3% of the 300 iterations) to achieve a more refined search in order to enhance the convergence of the algorithm in well placement optimization problems with discrete control variables. In this work, $\mathbb{A} = 100$ and $\mathbb{A} = 10$ is used for well placement and well control optimization levels, respectively. Haghighat Sefat, Elsheikh [37] recommended setting $0.1 \le \alpha_0 \le 0.5$ and c_{min} (i.e. when $k = k_{max}$) between 0.025 and 0.1 based on the complexity/noise of the search space. Initial sensitivity analysis in this work showed that faster convergence and more stable search process is achieved when $\alpha_0 = 0.5$ and $c_{min} = 0.08$ for both well location and control optimization.

Average SPSA: The expectation of the stochastically estimated gradient ($\hat{g}_k(u_k)$) is the true gradient due to the random nature of Δ_k [48]. Wang, Li [51], therefore, suggested using an averaged stochastic gradient calculated by use of an ensemble of perturbation vectors to improve the estimation of the search direction. Using the central difference formulation for gradient estimation, n_e independent samples of Δ_k are generated at each iteration, which results in $2 \times n_e$ objective function evaluations (Eq.(6)). The average stochastic gradient is then calculated by arithmetic averaging of the ensemble of n_p estimated gradients using the following equation:

$$\overline{\hat{g}_k(u_k)} = \frac{1}{n_e}\sum_{i=1}^{n_e} \hat{g}_i(u_k) \tag{9}$$

where $\overline{\hat{g}_k(u_k)}$ is the average stochastic gradient substituted for $\hat{g}_k(u_k)$ in Eq. (5). Note that developed framework is independent of the choice of the objective function. Variance or standard deviation can be added as an extra term to Eq. (9) to form a utility function if the objective is to reduce the risk while maximizing the objective value [37]. We observed that setting n_e between 3 to 5 provided a good quality of the estimated gradient at both the well placement and the well control levels.

1:1 perturbation allocation method: Uncertainty in reservoir description is generally captured by creating an ensemble (usually hundreds) of equally probable model realizations [2, 52]. Therefore, a fixed control vector (x) will produce different objective function values (J) when applied to different model realizations. Assuming n_c is a small subset of model realizations, selected as the representative of all available realizations, $2 \times n_e \times n_c$ function evaluations are generally required at each iteration to estimate $\overline{\hat{g}_k(u_k)}$ using n_p estimated gradients (Eq. (9)), which is referred to as all-to-all approach (Figure 1-Left) in this paper. Chen, Oliver [53] and Fonseca, Leeuwenburgh [35] showed that a 1:1 approach (Figure 1-Right), by mapping one member of the ensemble of control variables perturbations to one member of the ensemble of selected model realizations, can still provide a good estimate of the search direction at a significantly lower computation time while StoSAG [33] is used as the optimization algorithm (Note: StoSAG is an ensemble based optimization algorithm based on the EnOpt [53], where a smooth, stochastic approximated gradient is calculated using a temporal covariance matrix and an approximated simplex gradient over a number of perturbations of control variables). Assuming both ensembles of selected model realizations and control variables perturbations have an equal number of members ($n_c = n_e$) and considering that mean of the selected realizations is the objective function, a 1:1 approach can be used to reduce the number of function evaluations to $2 \times n_e$ in SPSA. Section 4.3 provides a comparison between all-to-all and 1:1 approach before employing the 1:1 approach in MSOF.

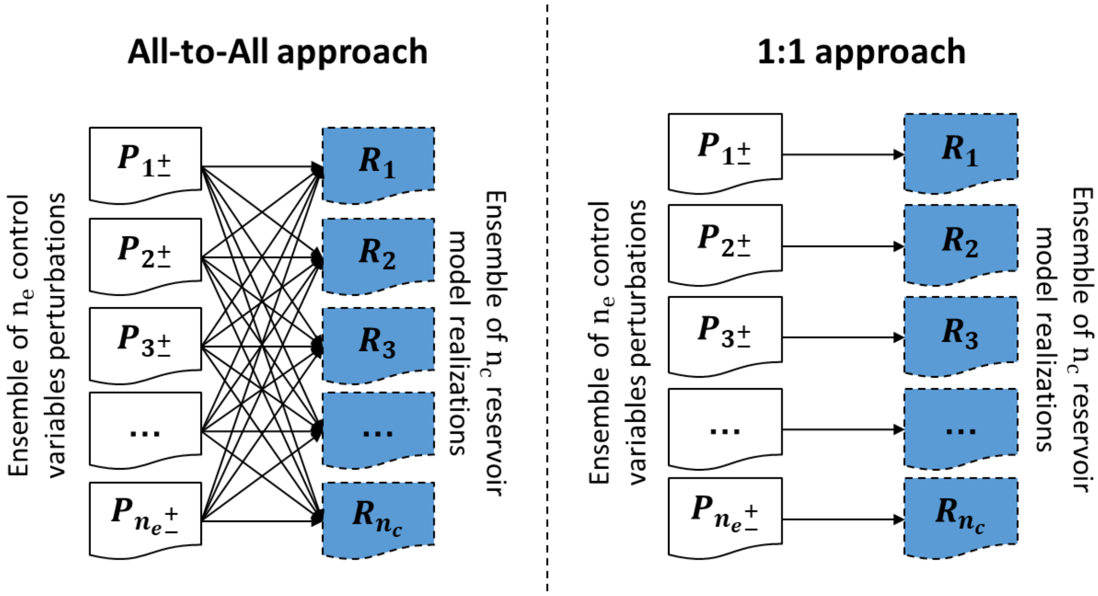

Figure 1-A schematic example for **Left:** all-to-all perturbation allocation method ($2 \times n_e \times n_c$ function evaluations are required at each iteration) **Right:** 1:1 method ($2 \times n_e$ function evaluations are required at each iteration). Note that central difference formulation is used for gradient estimation and both positive and negative perturbations are calculated using a particular realization.

3.2. Reservoir model realization selection

Selecting a small ensemble of model realizations as the representative of all available realizations can significantly reduce the computation time of robust optimization. A systematic approach is to tailor the realization selection process to the objective of the subsequent optimization stage. Wang, Echeverría-Ciaurri [2] proposed projecting all model realizations to 2D space while each dimension attributes to a time-varying (e.g. cumulative oil production) or static (e.g. permeability, oil-water contact, original oil in place) property of the model, followed by clustering and selecting representative realizations from each cluster. They used the normalized oil-water contact and the cumulative oil production as the model attributes when selecting representative realizations for well location optimization with the objective of maximizing NPV by enhancing reservoir sweep efficiency.

Haghighat Sefat, Elsheikh [37] proposed using the pairwise distance between water cut curves of all model realizations as similarity/dissimilarity measure when selecting realizations for well production optimization with the objective of increasing oil production by delaying water-breakthrough. Shirangi and Durlofsky [42] also proposed to measure similarity/dissimilarity between model realizations using a low-dimensional feature vector containing a combination of static and dynamic (varying with time) model properties, tailored to the optimization objectives. They found that both static and dynamic model properties need to be considered when selecting realizations for well location optimization while dynamic properties become especially important in realization selection for well control optimization.

Well placement optimization: Optimal well locations are often functions of both static (geological) and dynamic (flow properties) features of the reservoir, hence at the well placement optimization level, the realization selection is performed by creating a two-dimensional map where each model realization is characterized by its normalized permeability distance and the area under the field cumulative oil production curve. The permeability distance is defined as the Euclidean distance between the permeability field of a particular realization (m_i) and the average permeability field over all available realizations ($\overline{m}$) (i.e., $d_i = \|m_i - \overline{m}\|_2$ where $\|.\|$ represents the l_2-norm), which identifies the realizations showing different spatial permeability distribution compared to others. K-means clustering [54] is then performed to group all available realizations (n_r) into a small number of clusters (n_c) by iteratively finding the optimal cluster centers, i.e. $\tau_{opt} = \{\tau_1, \tau_2, \dots, \tau_{n_c}\}$, such that the summation of the distances of all n_r realizations from the nearest cluster center is minimized.

$$\tau_{opt} = \sum_{i=1}^{n_r} \min_{j=1,2,\dots,n_c} \left\|u_i - \tau_j\right\|^2 \tag{10}$$

where τ_j is the center for cluster j, and u_i denotes the mapped realization. Each realization is then assigned to the nearest cluster center. Determining the optimum number of clusters is an ill-posed problem and mostly involves some form of intuition supported by a performance measure. The Silhouette value [55] evaluates how well a data point is assigned to a particular cluster and is used as the clustering performance measure in this work. Assuming n_c clusters, the optimum number of clusters ($n_{c_{opt}}$) is determined by comparing the average silhouette value ($\overline{Sil}(n_c)$) for different numbers of clusters (n_c), where the maximum silhouette value indicates the best quality of clustering. Detailed information about the standard procedure of calculating average silhouette value can be found in Salehian, Sefat [12] and Haghighat Sefat, Elsheikh [37].

Well control optimization: The objective of the well control optimization level in this study is to improve oil recovery, which is typically achieved by delaying early water breakthrough in wells. Hence, following Haghighat Sefat, Elsheikh [37], the realization selection at the well control optimization level is performed by calculating the pairwise distance between model realizations as the summation of area between the well water cut versus production time curves of those realizations, given by:

$$D(m_i, m_j) = \sum_{g=1}^{n_p} \int_{t=0}^{t_f} \left(f_{wc_g}(m_i, t) - f_{wc_g}(m_j, t) \right) dt \tag{11}$$

where $f_{wc_g}(m_i, t)$ is the water cut in the g^{th} production well as a response of model i (m_i) at time t, n_p is the total number of production wells, and t_f is the final production time. The $n_r \times n_r$ dissimilarity matrix is then projected into two-dimensional space using multidimensional scaling (MDS) [56], preserving the Euclidean distance between data points in 2D as close as possible to the distance measured in the original space (Eq. (11)). K-means clustering followed by average silhouette value analysis is performed to group model realizations into $n_{c_{opt}}$ clusters, similar to the routine followed at the well placement optimization level. At both optimization levels, the realization closest to the center of each cluster is selected as the representative of that cluster (following Scheidt and Caers [57] and Haghighat Sefat, Elsheikh [37]). Note that if the number of selected realizations is larger than the number of clusters, then a weighted averaging approach should be used [37]. Section 4.2 compares the performance of the developed realization selection approach with the common alternatives.

3.3. Multi-Solution Optimization Framework (MSOF) for well placement and control

Fonseca, Leeuwenburgh [35] and Haghighat Sefat [9] showed that in optimization problems with a large number of control variables, the search space is characterized by several local optima with objective values close to each other. These local optima may form a multi-dimensional subspace where a minor change in the objective value is observed by varying control variables (similar to "mountain ridges") [9]. Although some of these solutions could be sub-optimal, they provide an acceptable level of improvement from operational point of view. Moreover the provided continuous, level of freedom, to achieve similar objective values using different sets of control variables, offers the much-needed operational flexibility. The developed MSOF explores the search space to identify multiple sets of solutions with distinctly different control variables but close-to-optimum objective values. The multiple sets of solutions can be considered as realizations of the (uncertain) control variables. A similar realization selection approach, as the one explained in section 3.2, can then be employed to select an ensemble of representative optimal solutions from each optimization level.

Solutions with low objective function values ($E(NPV)$) or with control variables values close to the optimal solution already selected are not good for the representative ensemble of optimal solutions from each optimization level. Hence, only the representative solutions with distinct differences in decision variables are selected from the top cases with objective values greater than a specified threshold, defined as $p\%$ of the maximum objective value (J_{max}) achieved. The optimal value of p ($p_{opt}\%$) depends on two competing criteria: distinct dissimilarity of the selected solutions, and proximity of the objective value of the selected cases to the maximum objective value. Selecting a large percentage of cases at each level (e.g. the extreme case of all cases) captures the maximum diversity between optimization scenarios. However, the selected cases do not all have the potential to achieve a close-to-optimum objective value after the next level of optimization and therefore do not qualify as an acceptable final solution. In this study, a sensitivity analysis followed by Salehian, Haghighat Sefat [45] showed that selecting $p_{opt} = 0.8$ at each optimization level (i.e. all cases with objective values in the range of $[p_{opt} \times J_{max}, J_{max}]$ are selected, where J_{max} denotes the maximum objective value achieved) provides the best performance in both sufficiently capturing the ensemble diversity and providing close-to-optimum objective values.

The similarity/dissimilarity of the selected solutions is measured as a pairwise distance between their corresponding control variable vectors, normalized into [0,1] using Eq. (4). At well placement optimization level, the employed approach calculates distances between reservoir grids with active wells irrespective of well names [45] while conventional Euclidean distance is used at the well control optimization level. The selected solutions are then projected onto two-dimensional space using MDS

[Note that the choice of the projection into 2-dimensional space is validated by performing the principal component analysis (PCA) [58] as explained in the results section] followed by k-means clustering, accompanied by average Silhouette analysis to identify the optimum number of clusters. One representative solution is then selected from each cluster, to be transferred to the next optimization level. Figure 2 shows the flow diagram of the robust multi-solution framework with well placement and control settings as the optimization levels.

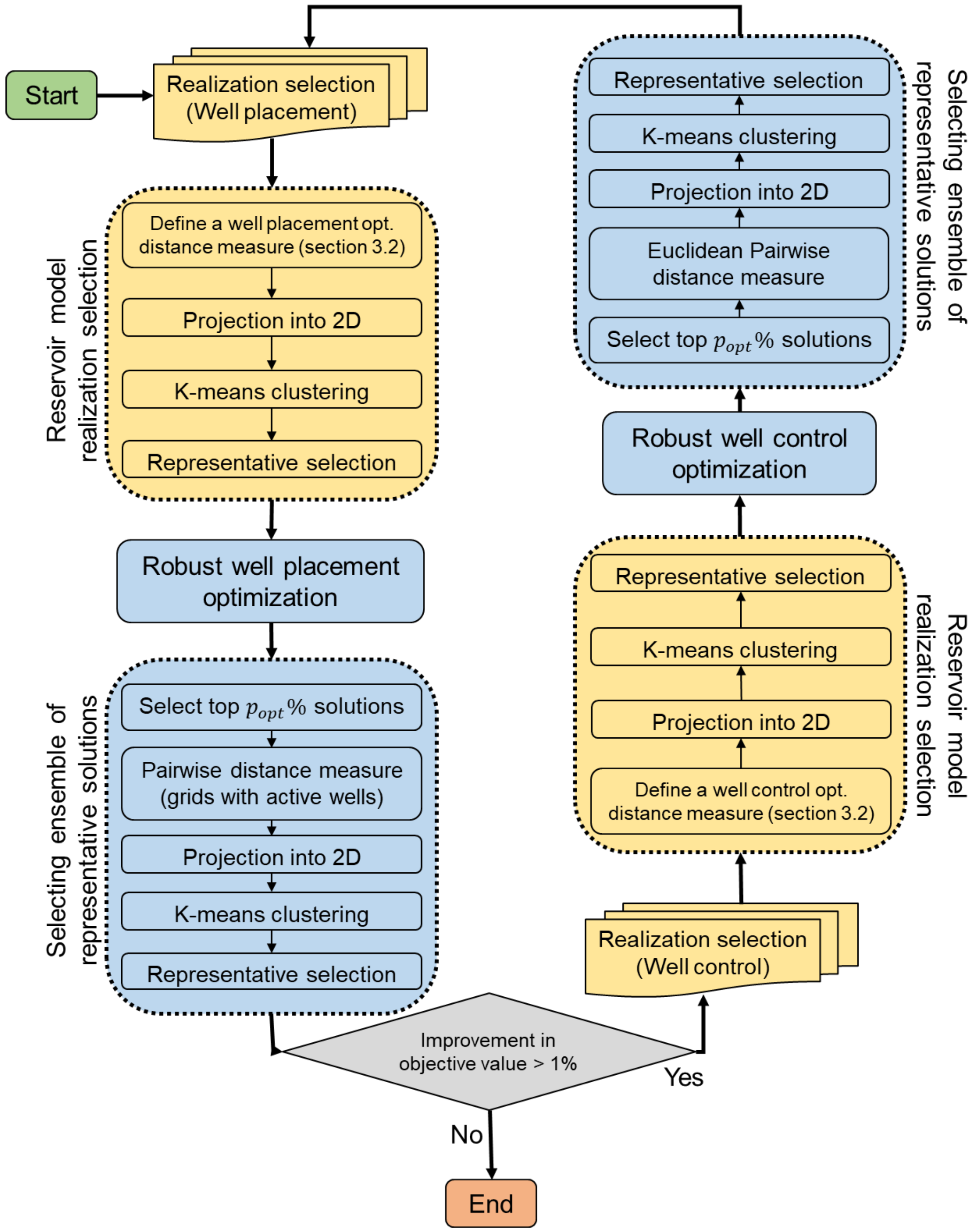

Figure 2-Flow diagram of the proposed robust, multi-solution optimization framework.

4. Case study – Brugge model

4.1. Model description and optimization settings

The Brugge (model) is a benchmark reservoir model based on a North Sea field [52]. The model consists of 139 × 48 × 9 (total of 60,048) grid blocks of which approximately 45,000 are active. The original model consists of 20 producers and 10 injectors. In this test case, five vertical producers and five vertical injectors are kept from the original model, due to the limited computational resources. The total production time is 30 years. Figure 3 shows the top structure of the model with the base case well locations. The uncertainty in the model description is quantified by 104 equiprobable realizations of the permeability, porosity, and net-to-gross (NTG) value distribution [59].

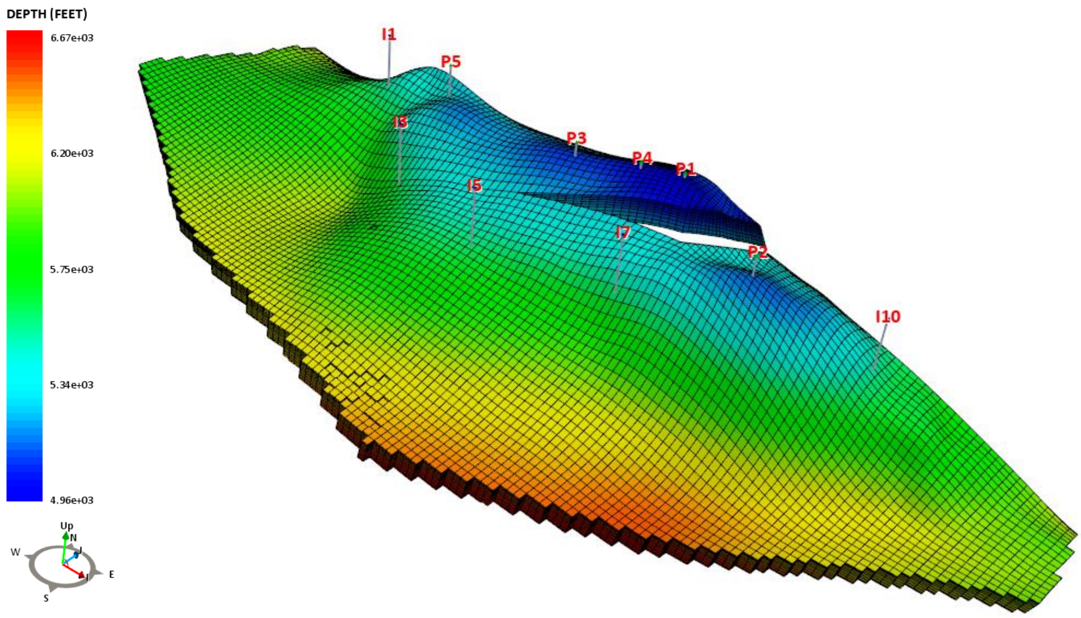

Figure 3-Top structure of the Brugge model.

The objective function, NPV (Eq. (1)), is calculated using the economic parameters provided in Table 1. 150 and 300 iterations are performed at well placement and control optimization levels, respectively. The top (i, j) location coordinates of the wells are optimized during the well location optimization level, which results in $10 \times 2 = 20$ control variables. A minimum inter-well distance constraint of $200\ m$ (equivalent to 2 grid blocks) is imposed during the well placement optimization level using a penalty method following Lu, Forouzanfar [22]. Well locations are maintained within the actual, irregular reservoir boundary limits, represented by a binary matrix with 0 and 1 elements indicating null and active reservoir grids, respectively. Following Salehian, Haghighat Sefat [45] each well is moved to the nearest active grid if it appears outside the reservoir boundaries during location optimization. The producers are all controlled by the Bottom Hole Pressure (BHP) varying between 725 and $1595\ psi$, while the injectors are each controlled by the water injection rate varying between 0 and $6289\ STB/day$. The producers are shut when their water cut exceeds the economic value of 90% calculated using Table 1 economic parameters. 30 control steps (of 1 year each) are considered during the well production/injection (control) optimization level resulting in the total of $30 \times 10 = 300$ control variables.

Table 1-Economic parameters for calculating NPV

Parameter	Value
Oil price	50 USD/STB
Water production cost	6 USD/STB
Water injection cost	3 USD/STB
Yearly discount rate	10%

4.2. Comparison of realization selection strategies

An ideal realization selection strategy should select the minimum number of realizations, as the representative of all realizations, which have the potential to provide a robust well placement and control scenario with optimal global performance during the subsequent optimization. The following realization selection strategies are compared in the context of the single-solution iterative sequential optimization approach:

1. No selections: optimization over full ensemble (104 in here) of model realizations.
2. The earlier-proposed systematic clustering approach tailored to the objective of subsequent optimization level.
3. The Reduced Random Sampling Strategy (RRSS), i.e. random selection of an ensemble of model realizations at each iteration proposed by Jesmani, Jafarpour [41].
4. A single realization corresponding to the P50 of NPV with the base case locations and control settings [60, 61].
5. A randomly selected single realization [39, 40].

Table 2 compares the global performance of different realization selection strategies while all other settings such as the number of iterations and the initial starting point of the optimization remain the same. Due to the stochastic nature of the SPSA algorithm, the comparison has been repeated with seven different random seeds and Figure 4 compares the average of the 7 runs. The full ensemble optimization (approach 1) delivers the maximum improvement at a significantly high computation cost, previously reported by e.g. van Essen, Zandvliet [18]. The systematic clustering (approach 2) and the RRSS (approach 3) both outperform the single realization optimization, but the global performance reduces as compared to the full-ensemble due to selecting a limited number of realizations. This is in line with Park [62] and Haghighat Sefat, Elsheikh [37], who showed that the mean value of a quantity over a subset of realizations is not exactly equal to the mean value over all realizations, however, the selected subset of realizations shows a similar behavior to the full ensemble and the optimal solution calculated using that subset provides close objective value as compared to the full ensemble optimization. The systematic clustering achieves greater global performance confirming that random sampling cannot completely capture the underlying uncertainty, even after randomly selected realizations are updated at each iteration in RRSS. Note that an ensemble of 4 and 5 model realizations was selected at the well placement and control optimization levels, respectively, when using the systematic clustering (See Figure 6 and Figure 12 in section 4.4). Following the recommendation by Jesmani, Jafarpour [41], RRSS was performed with 5 randomly selected model realizations at each iteration. Hence in this case, systematic clustering resulted in a lower computational cost at the well placement optimization level

Table 2- Global optimization performance (i.e. expected objective value and standard deviation over all realizations) using different realization selection strategies.

		No selection (full ensemble)		Proposed systematic clustering approach		Reduced Random Sampling Strategy (RRSS)		Single realization selection (P50)		Random selected single realization	
Well Placement Optimization	Number of simulations	31200		1350		1650		1650		1650	
		$E(NPV) \times 10^9$	$\sigma(E(NPV)) \times 10^8$	$E(NPV) \times 10^9$	$\sigma(E(NPV)) \times 10^8$	$E(NPV) \times 10^9$	$\sigma(E(NPV)) \times 10^8$	$E(NPV) \times 10^9$	$\sigma(E(NPV)) \times 10^8$	$E(NPV) \times 10^9$	$\sigma(E(NPV)) \times 10^8$
	Seed 1	2.39	0.71	2.30	3.64	2.30	3.23	2.24	10.07	2.21	11.55
	Seed 2	2.36	0.73	2.29	3.63	2.28	3.36	2.21	10.11	2.19	11.49
	Seed 3	2.40	0.73	2.32	3.67	2.29	3.12	2.21	10.18	2.18	11.74
	Seed 4	2.37	0.77	2.33	3.54	2.25	3.48	2.20	10.10	2.15	11.6
	Seed 5	2.36	0.72	2.31	3.70	2.24	3.25	2.19	10.11	2.22	11.63
	Seed 6	2.36	0.73	2.28	3.66	2.25	3.24	2.22	10.06	2.16	11.59
	Seed 7	2.41	0.71	2.32	3.49	2.27	3.14	2.21	10.03	2.14	11.31
	Average	2.38	0.73	2.31	3.62	2.27	3.26	2.21	10.09	2.18	11.56
Well Control Optimization	Number of simulations	62400		3300		3300		3300		3300	
		$E(NPV) \times 10^9$	$\sigma(E(NPV)) \times 10^8$	$E(NPV) \times 10^9$	$\sigma(E(NPV)) \times 10^8$	$E(NPV) \times 10^9$	$\sigma(E(NPV)) \times 10^8$	$E(NPV) \times 10^9$	$\sigma(E(NPV)) \times 10^8$	$E(NPV) \times 10^9$	$\sigma(E(NPV)) \times 10^8$
	Seed 1	3.11	0.22	3.03	2.6	2.96	1.77	2.94	10.97	2.77	12.29
	Seed 2	3.09	0.17	3.01	2.64	2.95	1.9	2.92	10.92	2.73	12.76
	Seed 3	3.21	0.35	3.04	2.43	2.86	1.93	2.94	10.85	2.72	12.64
	Seed 4	3.05	0.20	2.99	2.48	2.97	2.03	2.84	10.87	2.73	12.76
	Seed 5	3.13	0.24	3.03	2.55	2.91	1.87	2.89	10.84	2.70	12.51
	Seed 6	3.12	0.29	2.99	2.6	2.96	1.86	2.88	11.00	2.68	12.58
	Seed 7	3.15	0.38	3.00	2.66	2.96	1.79	2.90	10.93	2.70	12.52
	Average	3.12	0.26	3.01	2.57	2.94	1.88	2.90	10.91	2.72	12.58

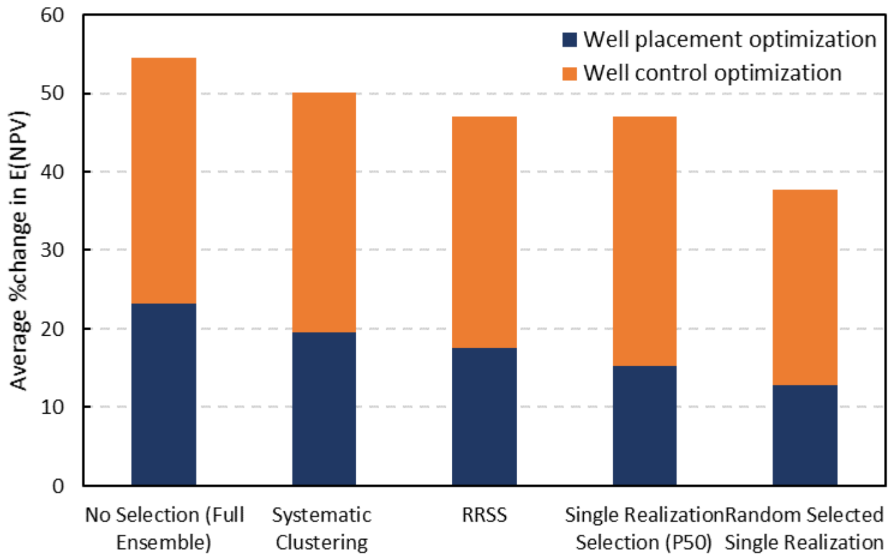

Figure 4-Average improvement in the expected objective value (over all realizations) as a result of well placement and control optimization using different realization selection strategies.

4.3. Comparison of 1:1 with all-to-all perturbation allocation in SPSA

As discussed in section 3.1, the following two approaches can be used when estimating the gradient of the expected objective value over an ensemble of model realizations using SPSA

- All-to-all: mapping each member of the ensemble of control variables' perturbations to all members of the ensemble of selected model realizations
- 1:1 method: mapping each member of the ensemble of control variables' perturbations to its single counterpart in the ensemble of selected model realizations.

Table 3 compares the performance of the two approaches at the well placement and control optimization level while all other settings, the number of iterations, selected realizations (using the systematic clustering approach), etc. remain the same. The lower improvement in the objective value is due to the lower quality of the estimated gradient using the 1:1 approach. However, a significant reduction in the computation time is achieved (4650 vs 20250 simulations required). Hence, the 1:1 approach is employed in the MSOF due to the limited computational resources.

Table 3-Global optimization performance (i.e. over all realizations) using 1:1 and all-to-all perturbation allocation approaches.

		1:1 method	All-to-all method
Base case	$E(NPV) \times 10^9$	1.93	
well placement optimization	$E(NPV) \times 10^9$	2.30	2.42
	Number of simulations	1350	4950
Well control optimization	$E(NPV) \times 10^9$	3.03	3.09
	Number of simulations	3300	15300

4.4. Application of MSOF for well placement and control optimization in the Brugge model

The MSOF along with the developed reservoir model realization selection techniques and 1:1 perturbation allocation method is applied to the Brugge model. Figure 5 shows the projection of all model realizations in 2D based on the normalized permeability distance and cumulative oil production. Note that the cumulative oil production is calculated based on the base case well locations and fully open control scenario (i.e. producers are set at minimum BHP and injectors are set at maximum rate). The optimum number of clusters is identified to be 4 ($n_{c_{opt}} = 4$) based on the average Silhouette analysis as the max value is achieved with four clusters (Figure 6). The realization closest to the center of each cluster is selected as the cluster representative (Figure 7) and the selected realizations are employed during the robust, well location optimization level.

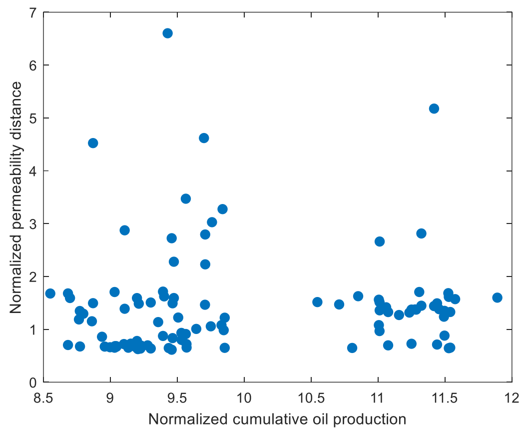

Figure 5-Two-dimensional map of all realizations based on permeability distance and cumulative oil production.

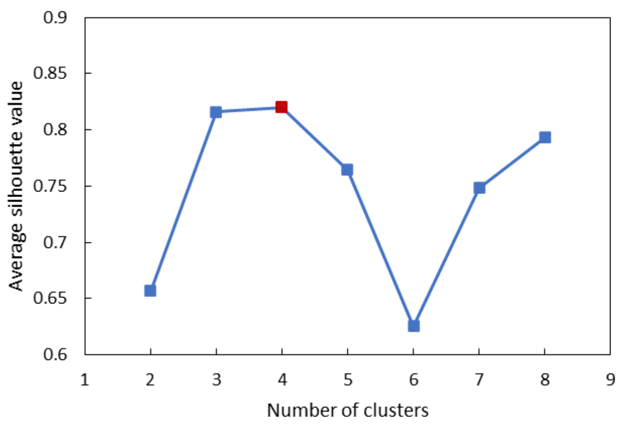

Figure 6-Average Silhouette value of all data points for different number of clusters in k-means.

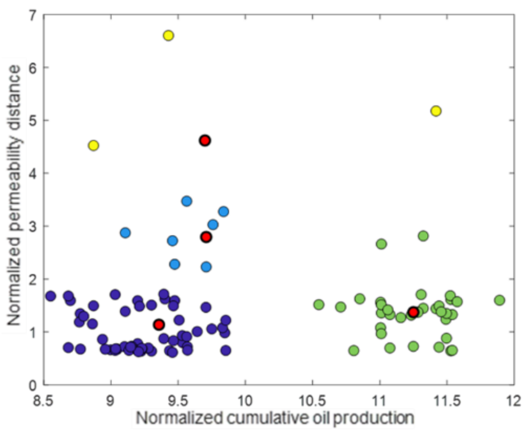

Figure 7-K-means clustering of reservoir model realizations considering four clusters, at well placement optimization level. Red points show the cluster representatives.

Figure 8 shows the improvement in the expected NPV ($E(NPV)$) of the selected realizations during well placement optimization iterations. The oscillations in the $E(NPV)$ are due to the minimum inter-well distance constraint imposed as a penalty term in the objective function definition (see Lu, Forouzanfar [22] for penalty term formulation). The dissimilarities between the top selected well location solutions, within an $E(NPV)$ shortfall of 20% as compared to the max case, are measured followed by projection on 2D using MDS (Figure 6). Note that PCA performed on the dissimilarity matrix of the selected well placement solutions showed that the first two dimensions account for approximately 70% of the variance in the original dataset of $N_x = 20$ dimensions. Hence, the relative distance between points in 2D space roughly represents the dissimilarity of the solution scenarios in the original space.

Each data point in Figure 9 represents a well location solution, with the color showing $E(NPV)$ over the selected realizations, confirming that a close to maximum objective value can be achieved by different well location solutions. The optimum number of clusters is identified to be 4 (Figure 10-left). The solution with the maximum NPV is selected as the representative of each cluster (shown by red points in Figure 10-right), considering the objective of choosing different solutions with highest objective values.

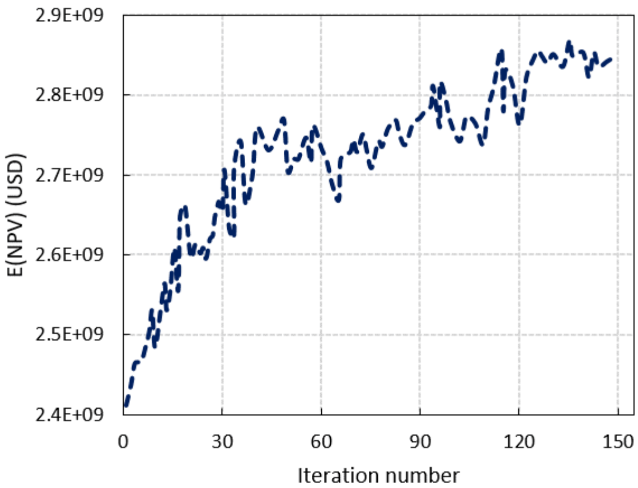

Figure 8-Expected objective value of the selected ensemble of realizations during well placement optimization.

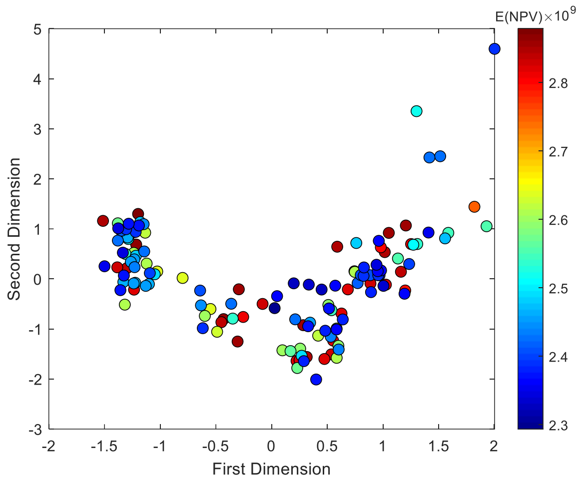

Figure 9-Projection of selected well location solutions, within an $E(NPV)$ shortfall of 20% as compared to the max case, into a two-dimensional space using MDS (color shows the objective value of each solution).

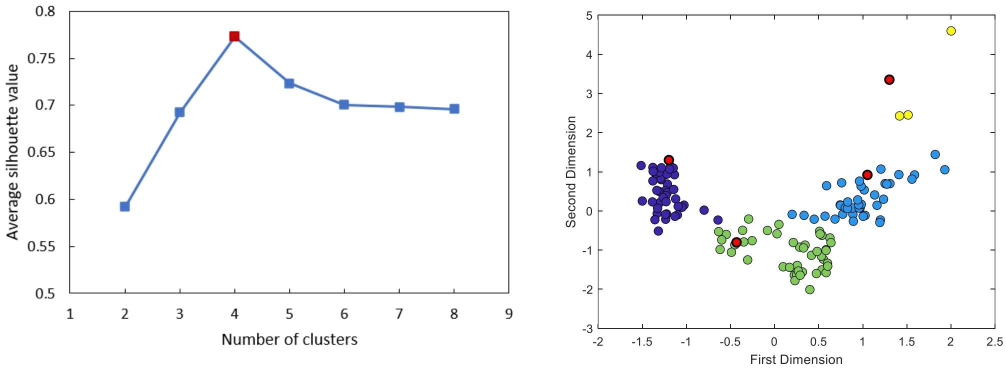

Figure 10- (Left)Mean Silhouette value analysis for the selected well placement solutions within an $E(NPV)$ shortfall of 20% as compared to the max case (Right) K-means clustering of the selected well placement solutions considering four clusters. Red points show the cluster representatives.

Figure 11 shows the representative well placement solutions, named L_1, L_3, L_4, and L_{64}, where the subscripts denote ranking of the solutions based on their $E(NPV)$ over the selected ensemble of realizations. Note that the case with the maximum objective value (L_1), i.e. the obtained optimal solution using the classic single-solution approach, is automatically selected as a representative solution. Table 4 shows the corresponding expected objective value and standard deviation of the selected well placement solutions when applied to the full ensemble of model realizations. A very similar global performance is observed by the selected ensemble of solutions (Table 4) while they provide a reasonable degree of flexibility in the well locations (Figure 11). It should be noted that a suboptimal member of the selected ensemble of solutions (e.g. L_4 here) can potentially provide a better global performance over all realizations, showing the robustness of the developed multi-solution framework by more efficient exploration of the search space.

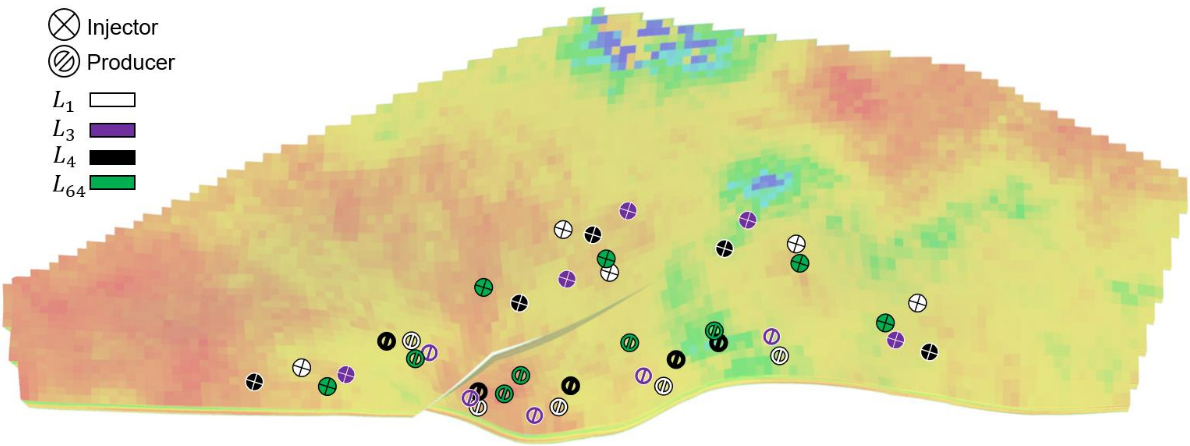

Figure 11-Four optimal well placement solutions obtained by MSOF.

Table 4-Mean and standard deviation of the optimal well placement solutions over all realizations.

Solution	$E(NPV) \times 10^9$	$\sigma(E(NPV)) \times 10^8$
Base Case	1.93	4.55
L_1	2.30	3.64
L_3	2.26	3.66
L_4	2.31	3.42
L_{64}	2.15	3.45

A new set of reservoir model realizations are selected, based on the distance measure described before (Eq. (11)), for each member of the ensemble of optimal well location solutions prior to well control optimization. Figure 12 shows the clustering performance, where the optimal number of clusters is determined using average Silhouette value analysis for each case. Note that the well water cut variation over time is a function of well location, resulting in different subsets of representative realizations to be selected for each optimal well location scenario (Figure 12). The control settings for each optimal well location solutions are then individually optimized at the next optimization level. Figure 13 shows improvement in the $E(NPV)$ of the corresponding ensemble of reservoir model realizations during 300 iterations of well control optimization for each optimal well location solution.

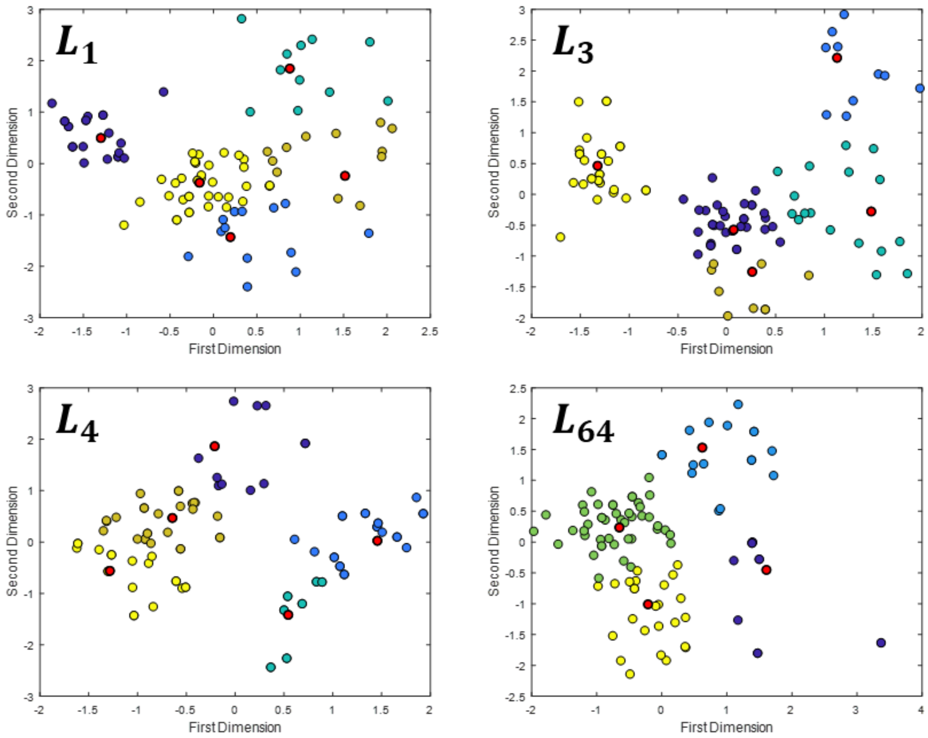

Figure 12- K-means clustering for reservoir model realization selection for each member of the ensemble of optimal well location solutions prior to well control optimization. Red points show the cluster representatives.

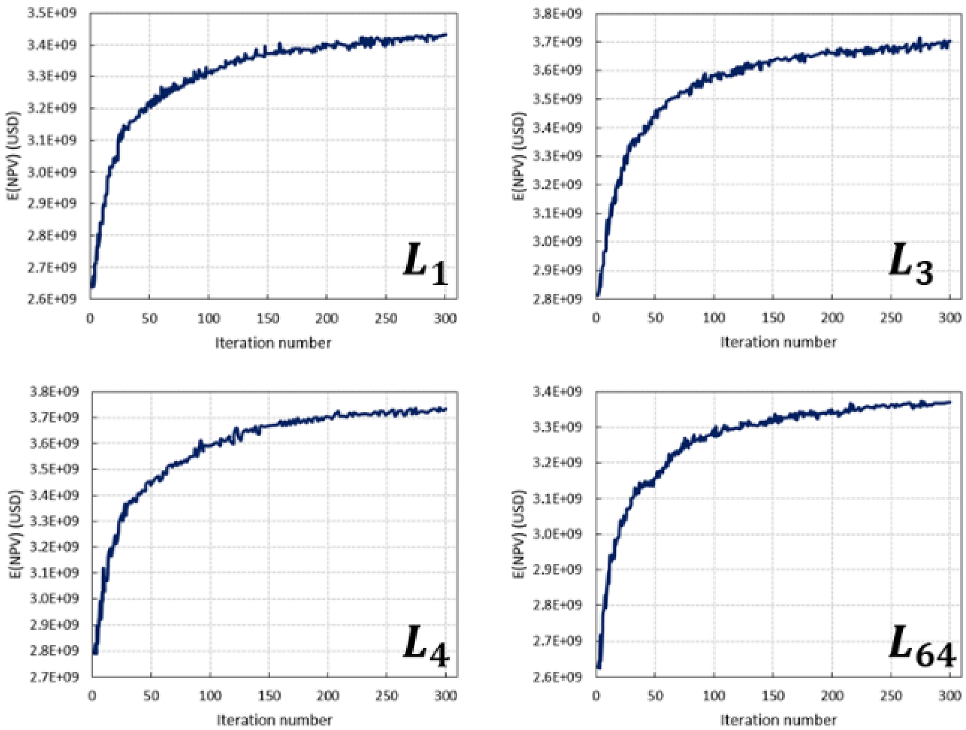

Figure 13- E(NPV) of the corresponding ensemble of reservoir model realizations during well control optimization for each optimal well placement scenario.

A similar clustering approach is applied to the control solutions where an ensemble of representative solutions is selected from the top cases within the $E(NPV)$ shortfall of less than 20% w.r.t. the max case. Conventional Euclidean distance is used to measure the dissimilarity between control scenarios followed by MDS to map them into two-dimensional space (Figure 14). Figure 15 shows the k-means clustering where the optimum number of clusters is determined by average Silhouette value analysis. The control scenario with the maximum NPV is then selected from each cluster as the representative of that cluster, resulting in a total of twelve optimal well control scenarios for all four well placement strategies.

The optimization trajectory as a result of using a gradient-based algorithm for optimizing well control settings (which are continuous variables) is clearly shown in Figure 14 while a more scattered search is performed during the well location optimization level with discrete variables (Figure 9). This feature of the optimization algorithm provides a level of freedom by exploring solutions around the optimal solution with limited exploration of new regions in the search space (i.e. capturing significantly different solutions). Further research is currently ongoing to achieve the maximum level of diversity in close-to-optimum solutions by enhancing the exploration of the search space, especially at the well location optimization level. At the well control optimization level a lower diversity of the selectable solutions is generally accepted due to the flexible nature of the well control operations.

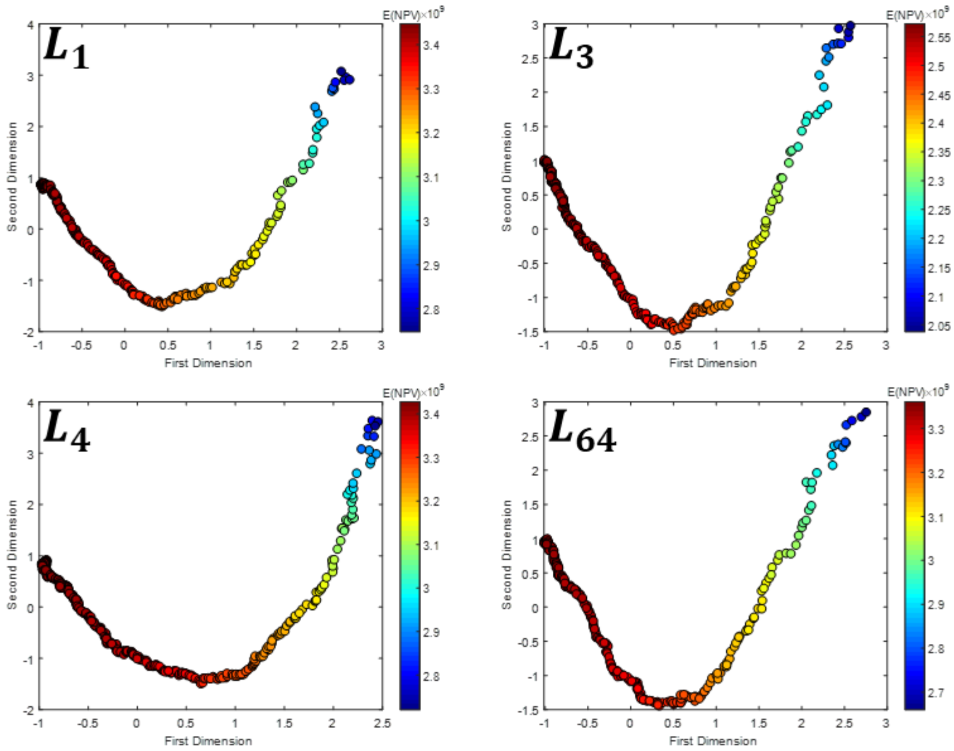

Figure 14- Projection of selected well control solutions (within an $E(NPV)$ shortfall of 20% as compared to the max case) corresponding to four optimal well locations into a two-dimensional space using MDS.

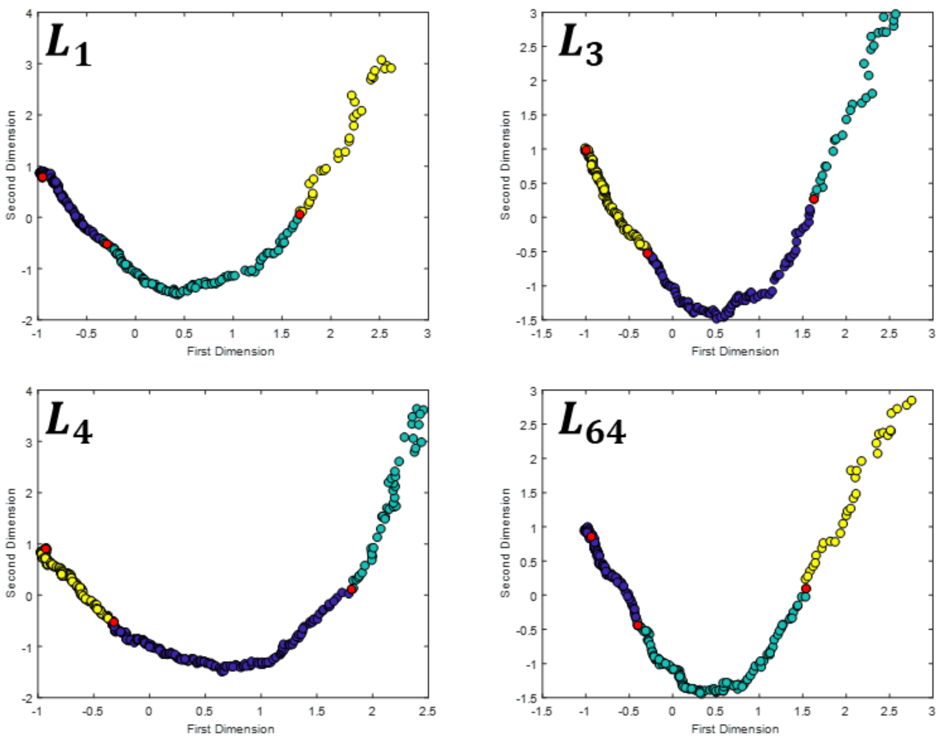

Figure 15 - K-means clustering followed by selection of the representative well control solutions, for each optimal well location. The optimal number of clusters for each ensemble is identified by average Silhouette value analysis.

Table 5 shows the mean of the final ensemble of close-to-optimum scenarios over all realizations, where e.g. $L_3.C_{268}$ denotes the 268th control scenario, ranked based on $E(NPV)$ during the well control optimization, using well location solution L_3. It can be seen that $L_4.C_{231}$ delivers the greatest global performance (over all reservoir model realizations) while only $L_1.C_1$ would be obtained as the single optimal solution using traditional, single-solution-transfer optimization frameworks. Moreover, a sub-optimal control scenario (i.e. with lower expected objective function value over the selected ensemble of realizations) could deliver higher global performance (over the full ensemble of realizations) (e.g. $E(NPV)_{L_1.C_{154}} > E(NPV)_{L_1.C_1}$ and $E(NPV)_{L_4.C_{231}} > E(NPV)_{L_4.C_1}$), demonstrating the robustness of the developed MSOF and its efficiency in the exploration of the search space.

The sequential optimization loop was terminated since no further improvements in the expected objective value were achieved at the second loop. $L_1.C_{154}$, $L_3.C_{150}$, $L_4.C_{231}$, and $L_{64}.C_1$ are selected as the optimal control scenarios with the highest $E(NPV)$ for each well location solution. A realistic level of variability in the optimal location and control is observed while the objective value varies in a relatively small range [2.80×10^9 - 3.08×10^9 USD], indicating the possibility of achieving a close-to-optimum objective value via different field development/control scenarios.

Table 5- Mean and standard deviation of the optimal solutions over all realizations.

Solution	$E(NPV) \times 10^9$	$\sigma(E(NPV)) \times 10^8$
$L_1.C_1$	3.03	2.60
$L_1.C_{154}$	3.00	2.59

$L_1.C_{265}$	2.78	2.42
$L_3.C_1$	2.84	2.56
$L_3.C_{150}$	2.93	2.71
$L_3.C_{268}$	2.70	2.39
$L_4.C_1$	2.88	2.71
$L_4.C_{231}$	3.08	2.76
$L_4.C_{246}$	2.85	2.45
$L_{64}.C_1$	2.80	2.61
$L_{64}.C_{126}$	2.76	2.57
$L_{64}.C_{263}$	2.58	2.32

5. Conclusions

The operational flexibility is a significant challenge, which needs to be expanded for practical applications of the optimization frameworks. Multi-objective (pareto) optimization is recommended when the optimal solution is decided based on the relative importance of each of the objectives. However, for a single-objective optimization problem with multiple types of variables at different levels, this paper presents a robust multi-solution optimization framework to offer multiple, distinct robust field development and control scenarios through an efficient exploration of the search space. Systematic clustering techniques were developed to select an ensemble of realizations to capture the underlying model uncertainties, as well as an ensemble of solutions with enough differences in control variables but close-to-optimum objective values, at each optimization level. SPSA was employed in a multi-level, sequential, iterative approach to find optimal well placement and control scenarios. The proposed framework was applied to a representative benchmark case study.

- The systematic realization selection process, tailored to the objective of the subsequent optimization stage, outperformed the Reduced Random Sampling Strategy (RRSS) and single realization selection approaches in efficiently representing the characteristics of the full ensemble of realizations while significantly reducing the computation time of robust optimization. The distance measure needs to be redefined for other optimization problems with a different objective.
- Estimation of the stochastic gradients at each iteration using a 1:1 ratio between the ensemble of control variables perturbations and the ensemble of selected model realizations substantially reduced the computation time while providing similar objective values.
- Multiple optimal well placement and control solutions with close-to-optimum objective values but different decision variables were obtained. Moreover, it was found that selected suboptimal location/control solutions over a small subset of realizations can outdo the optimal one when applied to all realizations, highlighting the significance of here-developed MSOF in order to provide a more robust solution and the much-needed operational flexibility in the field development optimization problems.

6. Acknowledgments

Authors are thankful to the sponsors of the “Value from Advanced Wells II” Joint Industry Project at Heriot-Watt University for providing financial support and Schlumberger for allowing academic access to their software.

7. References

1. Al-Ismael, M., et al. *A Well Placement Optimization Constrained to Regional Pressure Balance*. in *SPE Europec featured at 80th EAGE Conference and Exhibition*. 2018. Society of Petroleum Engineers.
2. Wang, H., et al., *Optimal well placement under uncertainty using a retrospective optimization framework.* Spe Journal, 2012. **17**(01): p. 112-121.
3. Li, L. and B. Jafarpour, *A variable-control well placement optimization for improved reservoir development.* Computational Geosciences, 2012. **16**(4): p. 871-889.
4. Bergey, P., *Generative well pattern design—principles, implementation, and test on OLYMPUS challenge field development problem.* Computational Geosciences, 2019: p. 1-16.
5. Busby, D., F. Pivot, and A. Tadjer. *Use of data analytics to improve well placement optimization under uncertainty*. in *Abu Dhabi International Petroleum Exhibition & Conference*. 2017. OnePetro.
6. Lepphaille, M., et al. *Generative Well Pattern Design Applied to a Giant Mature Field Leads to the Identification of Major Drilling Expenditure Reduction Opportunity*. in *Abu Dhabi International Petroleum Exhibition & Conference*. 2020. OnePetro.
7. Lu, R. and A.C. Reynolds, *Joint Optimization of Well Locations, Types, Drilling Order, and Controls Given a Set of Potential Drilling Paths.* SPE Journal, 2020.
8. Jiang, S., W. Sun, and L.J. Durlofsky, *A data-space inversion procedure for well control optimization and closed-loop reservoir management.* Computational Geosciences, 2019: p. 1-19.
9. Haghighat Sefat, M., *Proactive optimisation of intelligent wells under uncertainty*. 2016, Heriot-Watt University.
10. de Brito, D.U. and L.J. Durlofsky, *Well control optimization using a two-step surrogate treatment.* Journal of Petroleum Science and Engineering, 2020. **187**: p. 106565.
11. de Brito, D.U. and L.J. Durlofsky, *Field development optimization using a sequence of surrogate treatments.* Computational Geosciences, 2021. **25**(1): p. 35-65.
12. Salehian, M., M.H. Sefat, and K. Muradov, *Robust Integrated Optimization of Well Placement and Control under Field Production Constraints.* Journal of Petroleum Science and Engineering, 2021: p. 108926.
13. Barros, E., P. Van den Hof, and J. Jansen, *Informed production optimization in hydrocarbon reservoirs.* Optimization and Engineering, 2020. **21**(1): p. 25-48.
14. Fonseca, R., et al., *Introduction to the special issue: Overview of OLYMPUS Optimization Benchmark Challenge*. 2020, Springer.
15. de Moraes, R.J., et al., *An efficient robust optimization workflow using multiscale simulation and stochastic gradients.* Journal of Petroleum Science and Engineering, 2019. **172**: p. 247-258.
16. Fonseca, R.M., A.C. Reynolds, and J.D. Jansen, *Generation of a Pareto front for a bi-objective water flooding optimization problem using approximate ensemble gradients.* Journal of Petroleum Science and Engineering, 2016. **147**: p. 249-260.
17. Brouwer, D.R. and J. Jansen. *Dynamic optimization of water flooding with smart wells using optimal control theory*. in *European petroleum conference*. 2002. OnePetro.
18. van Essen, G., et al., *Robust waterflooding optimization of multiple geological scenarios.* Spe Journal, 2009. **14**(01): p. 202-210.

19. Isebor, O.J., L.J. Durlofsky, and D.E. Ciaurri, *A derivative-free methodology with local and global search for the constrained joint optimization of well locations and controls.* Computational Geosciences, 2014. **18**(3-4): p. 463-482.
20. Shirangi, M.G., O. Volkov, and L.J. Durlofsky, *Joint optimization of economic project life and well controls.* SPE Journal, 2018. **23**(02): p. 482-497.
21. Lu, R. and A. Reynolds. *Joint Optimization of Well Locations, Types, Drilling Order and Controls Given a Set of Potential Drilling Paths*. in *SPE Reservoir Simulation Conference*. 2019. Society of Petroleum Engineers.
22. Lu, R., F. Forouzanfar, and A.C. Reynolds. *Bi-objective optimization of well placement and controls using stosag*. in *SPE Reservoir Simulation Conference*. 2017. Society of Petroleum Engineers.
23. Li, L., B. Jafarpour, and M.R. Mohammad-Khaninezhad, *A simultaneous perturbation stochastic approximation algorithm for coupled well placement and control optimization under geologic uncertainty.* Computational Geosciences, 2013. **17**(1): p. 167-188.
24. Forouzanfar, F., W.E. Poquioma, and A.C. Reynolds, *Simultaneous and sequential estimation of optimal placement and controls of wells with a covariance matrix adaptation algorithm.* SPE Journal, 2016. **21**(02): p. 501-521.
25. Güyagüler, B., et al., *Optimization of well placement in a Gulf of Mexico waterflooding project.* SPE Reservoir Evaluation & Engineering, 2002. **5**(03): p. 229-236.
26. Almeida, L.F., M.M. Vellasco, and M.A. Pacheco, *Optimization system for valve control in intelligent wells under uncertainties.* Journal of Petroleum Science and Engineering, 2010. **73**(1-2): p. 129-140.
27. Harb, A., H. Kassem, and K. Ghorayeb, *Black hole particle swarm optimization for well placement optimization.* Computational Geosciences, 2019: p. 1-22.
28. Sarma, P., K. Aziz, and L.J. Durlofsky. *Implementation of adjoint solution for optimal control of smart wells*. in *SPE reservoir simulation symposium*. 2005. Society of Petroleum Engineers.
29. Van Essen, G., P. Van den Hof, and J.-D. Jansen, *Hierarchical long-term and short-term production optimization.* SPE Journal, 2011. **16**(01): p. 191-199.
30. Zandvliet, M., et al., *Adjoint-based well-placement optimization under production constraints.* Spe Journal, 2008. **13**(04): p. 392-399.
31. Jansen, J.-D., R. Brouwer, and S.G. Douma. *Closed loop reservoir management*. in *SPE reservoir simulation symposium*. 2009. OnePetro.
32. Jansen, J.D., *Adjoint-based optimization of multi-phase flow through porous media–a review.* Computers & Fluids, 2011. **46**(1): p. 40-51.
33. Fonseca, R.R.M., et al., *A stochastic simplex approximate gradient (StoSAG) for optimization under uncertainty.* International Journal for Numerical Methods in Engineering, 2017. **109**(13): p. 1756-1776.
34. Zingg, D.W., M. Nemec, and T.H. Pulliam, *A comparative evaluation of genetic and gradient-based algorithms applied to aerodynamic optimization.* European Journal of Computational Mechanics/Revue Européenne de Mécanique Numérique, 2008. **17**(1-2): p. 103-126.
35. Fonseca, R., et al., *Ensemble-based hierarchical multi-objective production optimization of smart wells.* Computational Geosciences, 2014. **18**(3-4): p. 449-461.
36. Jesmani, M., et al. *Application of simultaneous perturbation stochastic approximation to well placement optimization under uncertainty*. in *ECMOR XV-15th European Conference on the Mathematics of Oil Recovery*. 2016. European Association of Geoscientists & Engineers.
37. Haghighat Sefat, M., et al., *Reservoir uncertainty tolerant, proactive control of intelligent wells.* Computational Geosciences, 2016. **20**(3): p. 655-676.
38. Lu, R., F. Forouzanfar, and A.C. Reynolds, *An efficient adaptive algorithm for robust control optimization using StoSAG.* Journal of Petroleum Science and Engineering, 2017. **159**: p. 314-330.

39. Guyaguler, B. and R.N. Horne. *Uncertainty assessment of well placement optimization*. in *SPE annual technical conference and exhibition*. 2001. Society of Petroleum Engineers.
40. Chen, C., G. Li, and A. Reynolds, *Robust constrained optimization of short-and long-term net present value for closed-loop reservoir management.* SPE Journal, 2012. **17**(03): p. 849-864.
41. Jesmani, M., et al., *A reduced random sampling strategy for fast robust well placement optimization.* Journal of Petroleum Science and Engineering, 2020. **184**: p. 106414.
42. Shirangi, M.G. and L.J. Durlofsky, *A general method to select representative models for decision making and optimization under uncertainty.* Computers & geosciences, 2016. **96**: p. 109-123.
43. Li, G. and A.C. Reynolds, *Uncertainty quantification of reservoir performance predictions using a stochastic optimization algorithm.* Computational Geosciences, 2011. **15**(3): p. 451-462.
44. Gao, G., G. Li, and A.C. Reynolds. *A stochastic optimization algorithm for automatic history matching*. in *SPE annual technical conference and exhibition*. 2004. Society of Petroleum Engineers.
45. Salehian, M., M. Haghighat Sefat, and K. Muradov, *A Multi-Solution Optimization Framework for Well Placement and Control* SPE Reservoir Evaluation & Engineering, 2020.
46. Isebor, O.J. and L.J. Durlofsky, *Biobjective optimization for general oil field development.* Journal of Petroleum Science and Engineering, 2014. **119**: p. 123-138.
47. Schlumberger, *ECLIPSE® User Manual.* 2017.
48. Spall, J.C., *Multivariate stochastic approximation using a simultaneous perturbation gradient approximation.* IEEE transactions on automatic control, 1992. **37**(3): p. 332-341.
49. Spall, J.C., *Implementation of the simultaneous perturbation algorithm for stochastic optimization.* IEEE Transactions on aerospace and electronic systems, 1998. **34**(3): p. 817-823.
50. Spall, J.C., *Introduction to stochastic search and optimization: estimation, simulation, and control*. Vol. 65. 2005: John Wiley & Sons.
51. Wang, C., G. Li, and A.C. Reynolds, *Production optimization in closed-loop reservoir management.* SPE journal, 2009. **14**(03): p. 506-523.
52. Peters, L., et al., *Results of the Brugge benchmark study for flooding optimization and history matching.* SPE Reservoir Evaluation & Engineering, 2010. **13**(03): p. 391-405.
53. Chen, Y., D.S. Oliver, and D. Zhang, *Efficient ensemble-based closed-loop production optimization.* SPE Journal, 2009. **14**(04): p. 634-645.
54. Seber, G.A., *Multivariate observations*. Vol. 252. 2009: John Wiley & Sons.
55. Rousseeuw, P.J., *Silhouettes: a graphical aid to the interpretation and validation of cluster analysis.* Journal of computational and applied mathematics, 1987. **20**: p. 53-65.
56. Borg, I. and P. Groenen, *Modern multidimensional scaling: Theory and applications.* Journal of Educational Measurement, 2003. **40**(3): p. 277-280.
57. Scheidt, C. and J. Caers, *Uncertainty quantification in reservoir performance using distances and kernel methods--application to a west africa deepwater turbidite reservoir.* SPE Journal, 2009. **14**(04): p. 680-692.
58. Wold, S., K. Esbensen, and P. Geladi, *Principal component analysis.* Chemometrics and intelligent laboratory systems, 1987. **2**(1-3): p. 37-52.
59. Peters, E., et al., *Extended Brugge benchmark case for history matching and water flooding optimization.* Computers & Geosciences, 2013. **50**: p. 16-24.
60. Yang, C., et al. *Robust optimization of SAGD operations under geological uncertainties*. in *SPE reservoir simulation symposium*. 2011. Society of Petroleum Engineers.
61. Thanh, H.V., et al., *Robust optimization of CO2 sequestration through a water alternating gas process under geological uncertainties in Cuu Long Basin, Vietnam.* Journal of Natural Gas Science and Engineering, 2020. **76**: p. 103208.
62. Park, K., *Modeling uncertainty in metric space*. 2011: Stanford University.